DOI: 10.13009/EUCASS2023-617
Aerospace Europe Conference 2023 – 10TH EUCASS – 9TH CEAS

Electric field simulation of FEEP thruster for CubeSat application

Jeongsik SHIN, Kyun Ho LEE*†, Jungwon KUK** and Han Seo KO****
** Sejong University*
05006 SEOUL, Republic of Korea
***SOLETOP*
34051 DAEJEON, Repubplic of Korea
****Sungkyunkwan University*
03063 SUWON, Republic of Korea
wjdtlr5453@sju.ac.kr - khlee0406@sejong.ac.kr - jwguk@soletop.co.kr - hanseoko@skku.edu
† Corresponding Author

Abstract
To design the Field Emission Electric Propulsion (FEEP) thrusters for the CubeSat application, this study proposes an improved theoretical model of the emission current-applied voltage characteristic for a needle emitter to enhance the accuracy of theoretical performance predictions. Next, to investigate an electric field behaviour of the needle emitter, the electric field simulation is performed and predicted the emission current and onset voltage of the emitter, which are validated by comparing with the theoretical model and experimental measurements. Thus, we expect that the present models and methodologies will be useful to enhance the design reliability of the FEEP thrusters.

Nomenclature

e	Elementary charge	ε_0	Electric constant
m_e	Ion atom mass	I_{em}	Emission current
γ	Surface tension	R	Capillary emitter radius
α_T	Taylor cone half angle	R_{em}	Needle emitter tip radius
V	Voltage	r_{base}	Taylor cone base radius
V_{0x}	Extinction voltage	E	Electric field
V_0	Onset voltage	f	Thrust factor
d	Emitter tip to extractor distance	F	Thrust

1. Introduction

In recent times, with the increasing complexity and diversification of the CubeSat applications, there has been a development of various propulsion types specifically designed for the CubeSats[1]. Among these, the Field Emission Electric Propulsion (FEEP) thruster stands out due to its advantages such as simplicity, compact size, and high efficiency. As the FEEP system technologies have been investigated dominantly by a few European research groups[2] over several decades, it remains challenging for other researchers with no sufficient experience to directly apply their specialized outcomes when developing their own FEEP thrusters. To investigate the core technologies of the FEEP system and set up useful design methodologies, first, this study proposes an improved theoretical model of the emission current-applied voltage characteristic for an externally-wetted needle emitter to enhance the accuracy of theoretical performance predictions. Next, to investigate an electric field behaviour of the single needle emitter, the electric field simulation is performed to predict the emission current and onset voltage of the emitter. To verify a reliability of the simulation results, they are compared with the theoretical prediction and experimental measurements, which show good agreements.

DOI: 10.13009/EUCASS2023-617

Thus, we expect that the present models and methodologies will be useful to enhance the design reliability of the FEEP thrusters and prediction accuracies of their overall performance.

2. Theoretical Model

2.1 Previous Model

Since the 1980s, many theoretical models have been studied to predict the correlation between emission current and applied voltage for various types of emitter and liquid metal. Among them, the Mair's model[3] was derived based on the capillary emitter and liquid metal. The extinction voltage V_{0x} for the capillary emitter was expressed as:

$$\boldsymbol{V_{0x}} = \sqrt{\frac{2kR\gamma\cos\,(\alpha_T)}{\varepsilon_0}} \tag{1}$$

where the numerical constant k satisfies:

$$\boldsymbol{\hbar}\left(\frac{2d}{R}\right) < \boldsymbol{k} < \boldsymbol{\hbar}\left(\frac{4d}{R}\right) \tag{2}$$

For $(V/V_{0x} - 1) \ll 1$, Mair proposed the emission current I_{em} as:

$$\boldsymbol{I_{em}} = 3\pi\sqrt{\frac{2e}{m_e}}\frac{R\gamma\cos\,(\alpha_T)}{\sqrt{V_{0x}}}\left(\frac{V}{V_{0x}} - 1\right) \tag{3}$$

To derive the correlation between-applied voltage and emission current for the needle emitter, Tajmar[4] conducted a comparative study between the experimental and calculated results of the emission current using the theoretical model for the needle emitter. For this, the Tajmar's model was expressed as Eq. (4) and (5) for $(V/V_0 - 1) \ll 1$ based on the results that the Mair's model could be applied to the needle emitter with a low flow impedance[5].

$$\boldsymbol{I_{em}} = 3\pi\sqrt{\frac{2e}{m_e}}\frac{r_{base}\,\gamma\cos\,(\alpha_T)}{\sqrt{V_0}}\left(\frac{V}{V_0} - 1\right) \tag{4}$$

$$\boldsymbol{V_0} = \boldsymbol{\hbar}\left(\frac{2d}{r_{base}}\right) \times \sqrt{\frac{\gamma r_{base}}{\varepsilon_0}} \tag{5}$$

As shown in Figure 1, r_{base} is defined as the radius of the Taylor cone base formed at the needle emitter tip[6]:

$$\boldsymbol{r_{base}} = \boldsymbol{R_{em}\cos\,(\alpha_T)} \tag{6}$$

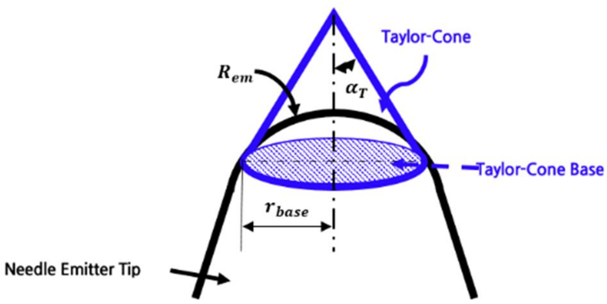

Figure 1: Taylor cone on needle emitter tip

DOI: 10.13009/EUCASS2023-617

2.2 Improved Theoretical Model

To check an accuracy of the previous model, the Tajmar's model and experimental measurements were compared for a single needle emitter and an indium propellant. As seen in Figure 2, some large deviation could be observed between the two results. While the Tajmar's model showed good agreements in the low emission current range below approximately 40 μA, the emission current predictions of the Tajmar's model were underestimated especially above 40 μA and the deviations between the two results became larger as the current increased.

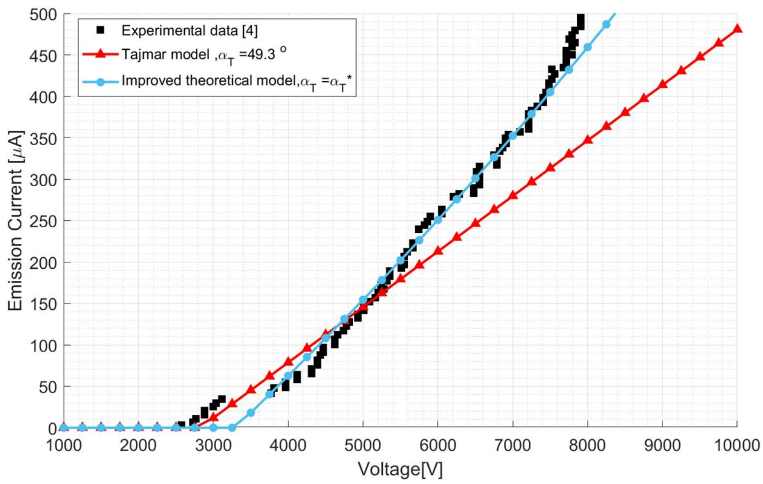

Figure 2: Comparisons of emission current-applied voltage characteristics for a single needle emitter

Hence, the present study performed some detailed investigations to find the causes of these deviations and improve the accuracy of the theoretical model as follows. First, we found some errors in the previous theoretical equations. In the Tajmar's model, Eq. (4) is expressed by simply replacing the parameters R and V_{0x} in Eq. (3) with r_{base} and V_0, respectively. Hence, we doubt that there would be a lack of mathematical plausibility since Eq. (4) was not directly derived for the needle emitter. Therefore, the present study derived a theoretical model for the needle emitter based on the mathematical derivation of the Mair's model, and then found to be expressed as the following equation:

$$\boldsymbol{I_{em}} = \boldsymbol{3\pi}\sqrt{\frac{\boldsymbol{2e}}{\boldsymbol{m_e}}}\frac{\boldsymbol{r_{base}\,\gamma\cos(\alpha_T)}}{\boldsymbol{2\sqrt{V}}}\left(\frac{\boldsymbol{V^2}}{\boldsymbol{V_{0x}^2}} - \boldsymbol{1}\right) \tag{7}$$

where r_{base} is defined by Eq. (6). For $(V/V_{0x} - 1) \ll 1$, Eq. (7) can be simplified to the following expression:

$$\boldsymbol{I_{em}} = \boldsymbol{3\pi}\sqrt{\frac{\boldsymbol{2e}}{\boldsymbol{m_e}}}\frac{\boldsymbol{r_{base}\,\gamma\cos(\alpha_T)}}{\boldsymbol{\sqrt{V}}}\left(\frac{\boldsymbol{V}}{\boldsymbol{V_{0x}}} - \boldsymbol{1}\right) \tag{8}$$

When comparing with Eq. (8), it was found that Eq. (4) of the Tajmar's model has some errors such as using $V_0^{1/2}$ and V/V_0 instead of $V^{1/2}$ and V/V_{0x}. Second, both the Mair's and Tajmar's models have proposed and used the simplified models of Eq. (3) and (4) with the assumption of $(V/V_{0x} - 1) \ll 1$. However, depending on the physical characteristics of various liquid metal propellants and the operating conditions of the FEEP thrusters, there is a possibility that $(V/V_{0x} - 1) \ll 1$ may not be valid for a reasonable assumption anymore. Hence, we concluded that the full equation of Eq. (7) is more suitable because the previous simplified models have a radical limitation to applying to the nominal operating conditions of the FEEP thrusters in the high voltage ranges over several kV. Third, Taylor[7] derived theoretically that the Taylor cone half angle forms 49.3° when the electrostatic force balances the surface tension of the liquid metal, and Driesel *et al.*[8] found that the Taylor cone half angle gradually decreased as the applied voltage increased. However, both the Mair's and Tajmar's models adopted conventionally this constant value to Eq. (3) and (4) over the entire emission current-voltage ranges in their previous studies without considering this relation. Instead, we decided that an optimal value of the Taylor cone half angle needs to be evaluated other than the conventional 49.3° at which the Taylor cone formed.
As a result, we can propose an improved theoretical model by deriving the emission current-applied voltage relation from Eq. (6) ~ (7) and the optimal value of the Taylor cone half angle by comparing with the experimental

DOI: 10.13009/EUCASS2023-617

measurements of the emission current-applied voltage characteristic. To verify the accuracy of the present improved model, its predictions of the emission current-applied voltage are compared in Figure 2 with the experimental measurements and the previous model's data. It is observed that the improved theoretical model exhibited more similar predictions with a high accuracy especially in the high emission current regions above approximately 40 μA. When considering the nominal emission current values of the FEEP thrusters are typically over 100 μA, we expect that the present improved theoretical model can yield more accurate predictions than the previous models.

3. Electric Field Simulation

Next, we set up an electric field simulation model to calculate numerically the electric field distribution of the FEEP thruster by solving Laplace's equation depending on the voltage condition applied to the emitter and the extractor using finite element and boundary element methods:

$$\boldsymbol{\nabla} \cdot \boldsymbol{E} = \mathbf{0} \tag{10}$$

An overall flowchart of the electric field simulation is described in Figure 3. The electric field simulation model proposed in this study not only calculates the electric field behavior of the FEEP thrusters but also can predict the emission current-applied voltage characteristic by using the electric field value estimated from the simulation result.

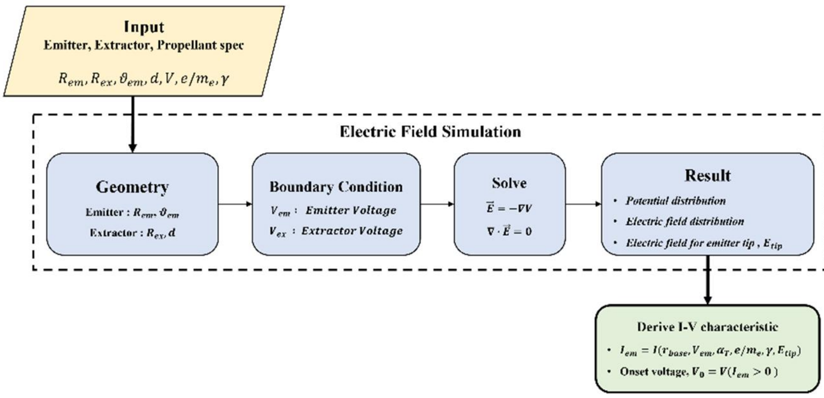

Figure 3: Flowchart of electric field simulation

Using this model, we performed the electric field simulation for a single needle emitter[4] with a 2-D axisymmetric domain. The electric field distribution of the single needle emitter is illustrated in Figure 4, which shows that the estimated electric field originates from the emitter and directs toward the extractor. While the electric field levels of most simulation regions seem to remain below approximately 10^7 V/m, an especially higher electric field of about 10^9 V/m is concentrated at the emitter tip due to its sharpness.

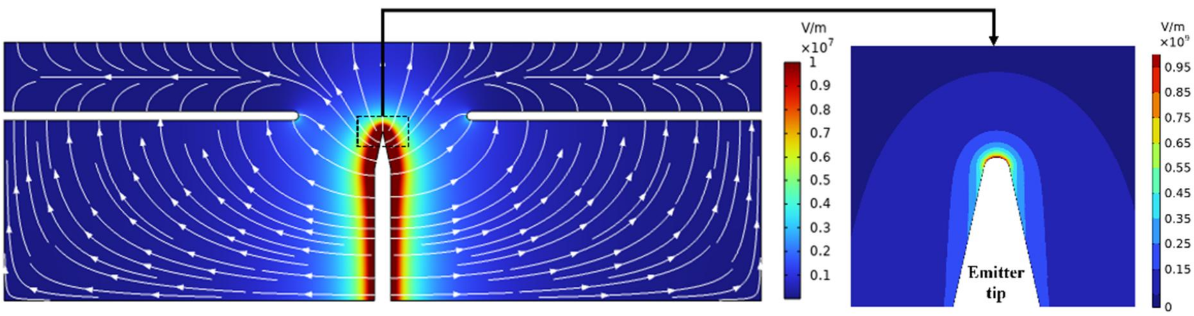

Figure 4: Electric field distribution for a single needle emitter

Figure 5 presents a comparison of the emission current-applied voltage characteristics between the electric field simulation result and experimental data[4] for the single needle emitter. For an initial calculation, the Taylor cone half

DOI: 10.13009/EUCASS2023-617

angle(α_T) was assumed to be 49.3° and the electric field value estimated at the emitter tip (E_{tip}) was used as a representative electric field value. The simulation model exhibits a reasonable agreement with the experimental data, particularly showing a nearly identical profile in the low emission current region (≤ 40 μA).

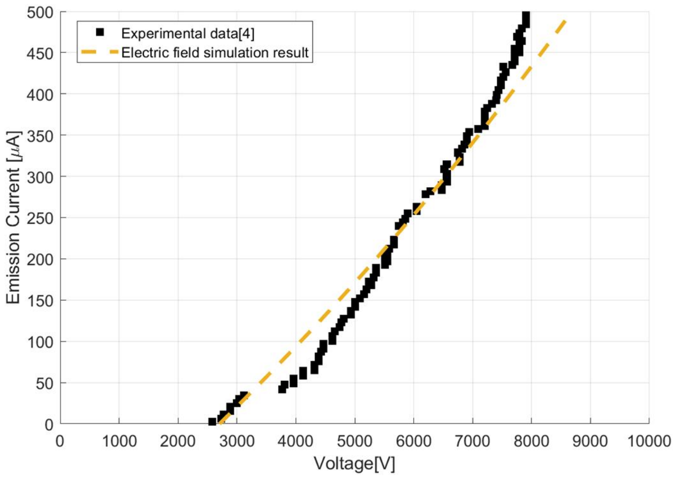

Figure 5: Comparison of emission current-applied voltage characteristics between simulation and experiment[4]

In addition, the onset voltage value deduced from the simulation model is compared in Table 1 with the theoretical value obtained from Eq. (5) and the experimental measurement. Through a comparison of the relative errors for the experimental value, it was found that the onset voltage value estimated from the electric field simulation model closely matched the experimental data. Hence, we could verify the accuracy and reliability of the present electric field simulation model.

Table 1: Comparison of onset voltage values

Emitter type	**Experimental value[4]**	**Theoretical value of Eq. (5) (Relative error)**	**Electric field simulation value (Relative error)**
Externally wetted needle emitter	2730	2820 (3.3 %)	2710 (0.7 %)

4. Performance comparison

A thrust of the FEEP thruster is expressed as the following equation[2]:

$$\boldsymbol{F = I_{em}\sqrt{2V\frac{m_e}{e}}\cdot f} \qquad \textbf{(11)}$$

where f is the thrust coefficient representing the effect of ion beam divergence as a percentage of thrust. As seen in Eq. (11), the thrust is proportional to I_{em} and $V^{1/2}$, which indicates that the performance of the FEEP thruster is affected by the emission current-applied voltage characteristic. The thrust-applied voltage characteristics are depicted in Figure 6 for the experimental measurements and the emission current values calculated from the theoretical models. In particular, when referring to the nominal operating condition of the commercial FEEP thruster, it is necessary to apply a voltage of approximately 6 kV or higher to generate substantial thrust[2]. We could find that the improved theoretical model shows higher accuracies than the Tajmar's model, especially in a relatively larger thrust region above about 2.4 μN. Figure 6 also presents the thrust-applied voltage characteristic obtained from the electric field simulation. We could found that the electric field simulation result exhibits a reasonable agreement with the experimental data value over the entire thrust-applied voltage characteristic range.

DOI: 10.13009/EUCASS2023-617

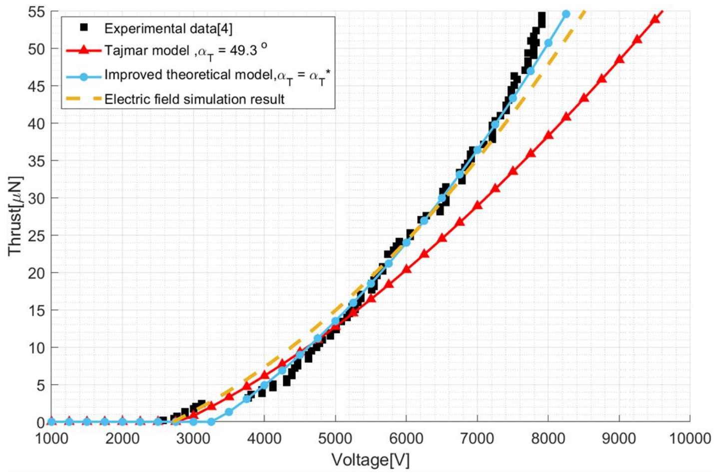

Figure 6: Comparisons of thrust-applied voltage characteristics for a single needle emitter

5. Conclusion

The emission current-applied voltage characteristic of the FEEP thrusters is crucial in its design process, as it directly influences its overall performance. Through the utilization of the improved theoretical model and the electric field simulation model established by the present study, we could obtain more accurate predictions of the emission current-applied voltage characteristics than the previous model when compared with the experimental measurements, especially in the higher emission current regions. As a result, we could also estimate the thrust performance of the FEEP thrusters more precisely. For further improvement, various attempts are underway to estimate the proper value of the representative electric field instead of simply using the E_{tip} . Consequently, we anticipate that the present theoretical models will be instrumental in estimating and evaluating the proper design outcomes of a new FEEP thruster currently under development.

Acknowledgement

This work was supported by Space Challenge Project (NRF-2021M1A3B8078958) and Future Space Navigation & Satellite Research Center Program (NRF-2022M1A3C20 74404) through the National Research Foundation funded by the Ministry of Science and ICT of Republic of Korea.

References

[1] Lee, K.H., Shin, J., Kim, H., Kuk, J.W., and Ko, H.S. 2021. Technology trends of cubesat propulsion system. In: *Proceedings of the 2021 Korean Society of Propulsion Engineers Fall Conference.* 511.

[2] Schönherr, T., Little, B.D., Reissner, A., and Seifert, B. 2019. Development , Production , and Testing of the IFM Nano FEEP Thruster. In: *36th International Electric Propulsion Conference*. 1–11.

[3] Mair, G.L.R. 1984. Theoretical determination of current-voltage curves for liquid metal ion sources. *Journal of Physics D: Applied Physics*. 17:2323–2330.

[4] Tajmar, M. 2005. Influence of Taylor cone size on droplet generation in an indium liquid metal ion source. *Applied Physics A*. 81:1447–1450.

[5] Mair, G. L. R. 1997. The effects of flow impedance on the current - voltage characteristics of liquid-metal ion sources. *Journal of Physics D: Applied Physics*. 30:1945–1950.

[6] Tajmar, M. 2005. Development of a Lifetime Prediction Model for Indium FEEP Thrusters. In: *41st AIAA/ASME/SAE/ASEE Joint Propulsion Conference and Exhibit*.

[7] Taylor, G. I. 1964. Disintegration of water drop in an electric field. *Proceedings of the Royal Society of London. Series A: Mathematical and Physical Sciences*. 280(1382):383–397.

[8] Driesel, W., Dietzsch, Ch., and Möser, M. 1996. In situ HV TEM observation of the tip shape of lead liquid metal ion sources. *Journal of Physics D: Applied Physics*. 29:2492–2500.